International Journal of Nanomedicine

Dovepress
open access to scientific and medical research

Open Access Full Text Article

ORIGINAL RESEARCH

Inhibitory effect of magnetic Fe_3O_4 nanoparticles coloaded with homoharringtonine on human leukemia cells in vivo and in vitro

This article was published in the following Dove Press journal:
International Journal of Nanomedicine
6 September 2016
Number of times this article has been viewed

Meiyu Chen[1–3,*]
Fei Xiong[4,5,*]
Liang Ma[1–3,*]
Hong Yao[1–3]
Qinrong Wang[1–3]
Lijun Wen[1–3]
Qian Wang[1–3]
Ning Gu[4,5]
Suning Chen[1–3]

[1]Jiangsu Institute of Hematology, The First Affiliated Hospital of Soochow University, Suzhou, [2]Key Laboratory of Thrombosis and Hemostasis of Ministry of Health, Collaborative Innovation Center of Hematology, Soochow University, Suzhou, [3]Collaborative Innovation Center of Hematology, Soochow University, Suzhou, [4]State Key Laboratory of Bioelectronics, Jiangsu Key Laboratory for Biomaterials and Devices, School of Biological Science and Medical Engineering, Southeast University, Nanjing, [5]Collaborative Innovation Center of Suzhou Nano Science and Technology, Suzhou, People's Republic of China

*These authors contributed equally to this work

Correspondence: Suning Chen
Jiangsu Institute of Hematology, The First Affiliated Hospital of Soochow University, Suzhou 215006, People's Republic of China
Email chensuning@sina.com

Ning Gu
State Key Laboratory of Bioelectronics, Jiangsu Key Laboratory for Biomaterials and Devices, Southeast University, Nanjing 210009, People's Republic of China
Email guning@seu.edu.cn

Abstract: Homoharringtonine (HHT), a natural cephalotaxine alkaloid, has been used in the People's Republic of China for treatment of leukemia for >3 decades. Here, we employed magnetic Fe_3O_4 nanoparticles (MNP-Fe_3O_4) to improve the therapeutic effect of HHT and investigated its biological effects. Within a certain range of concentrations, the HHT-MNP-Fe_3O_4 showed a more enhanced inhibitory effect on the selected myeloid leukemia cell lines than HHT alone. Compared with HHT, HHT-MNP-Fe_3O_4 could induce more extensive apoptosis in leukemia cells, which also showed more pronounced cell arrests at G0/G1 phase. HHT-MNP-Fe_3O_4 enhanced antitumor activity by downregulating myeloid cell leukemia-1, which could inhibit the activation of caspase-3 and poly-ADP-ribose polymerase. In vivo experiments using tumor-bearing animal models showed that the mean tumor volume with HHT-MNP-Fe_3O_4 was significantly smaller than that with HHT alone (193±26 mm^3 versus 457±100 mm^3, $P<0.05$), while the mean weight was 0.67±0.03 g versus 1.42±0.56 g ($P<0.05$). Immunohistochemical study showed fewer myeloid cell leukemia-1-stained cells in mice treated with HHT-MNP-Fe_3O_4 than with the controls. These findings provide a more efficient delivery system for HHT in the treatment of hematological malignancy.

Keywords: leukemia, magnetic nanoparticles, magnetic Fe_3O_4 nanoparticles, HHT

Introduction

Myeloid leukemia, a type of leukemia involving myeloid tissue, is a heterogeneous group of clonal disorders characterized by an abnormal proliferation of myeloid stem/progenitor cells and subsequent bone marrow failure. Although a majority of these patients can achieve complete remission by current chemotherapies, most of these patients may ultimately relapse within a certain limited period. Hence, there is a largely unsatisfied need for more effective drugs for the patient population with treatment failure or relapse.

Homoharringtonine (HHT), a kind of Chinese traditional medicine, is a compound derived from the *Cephalotaxus* genus.[1] HHT was first isolated in the 1970s and was found to have natural antitumor and antileukemic activities in in vitro and in vivo studies.[2,3] HHT was initially considered as one of the most effective choices for patients with acute myelocytic leukemia (AML) and chronic myelogenous leukemia (CML) who failed with interferon alpha (IFN-α) therapy and could not tolerate hematopoietic stem cell transplantation.[4,5] However, after the tyrosine kinase inhibitor imatinib mesylate was recommended as the standard therapy for patients with CML,[6] the attention toward HHT began to decrease.[7] Recently, a few encouraging findings demonstrated that HHT played a critical role in the treatment of patients who failed with imatinib therapy, especially those with tyrosine kinase inhibitor-insensitive T315I mutation.[8]

submit your manuscript | www.dovepress.com
Dovepress
http://dx.doi.org/10.2147/IJN.S105543

According to prior studies, HHT exerts functions probably in a unique way. HHT induced apoptosis of human myeloma cell lines by activating caspase-3 and mediating cleavage of poly-ADP-ribose polymerase (PARP). In addition, the expression of Bax is upregulated while that of Bcl-2 is slightly decreased.[9] Lou et al[10] demonstrated HHT-induced apoptosis through intrinsic and extrinsic apoptotic pathways, including the activation of caspase-3, caspase-8, caspase-9, and PARP. HHT may also inhibit the synthesis of short-lived proteins by targeting the A-site cleft of eukaryotic ribosomes.[11] The myeloid cell leukemia-1 (Mcl-1) protein, a member of anti-apoptotic Bcl-2 family proteins, is one of such short-lived proteins that are highly expressed in leukemia cells.[12]

As a promising antitumor agent, HHT, which is hydrophobic, must be formulated in solvents to increase the solubility and bioavailability. Unacceptable cardiovascular adverse events, including hypotension and tachycardia, may occur when patients are treated with HHT at a dose of 5 mg/m^2 or 6 mg/m^2 daily.[13,14] However, the efficacy of drugs is usually associated with dose- and duration-dependent side effects. With the rapid development of nanoscience, people started drawing attention to nanotechnology for cancer therapy and drug delivery for the purpose of enhanced drug accumulation and reduced dose.[15] Recent reviews promised a broad prospect for nanotechnology as a fundamental tool in cancer research.[16,17] In addition, polymer nanospheres and nanoparticles (NPs) have been increasingly proved to enhance the drug delivery efficiency to target cells.[18,19] By coloading with NPs, the increased solubility, decreased side effects, and extended availability in circulation were observed for chemotherapeutic agents. With the NPs, drug particles can be dispersed to increase the half-life in the blood and prevent protein from adsorption. Nanoparticle albumin-bound (nab) paclitaxel, a novel product in the NP field, combines paclitaxel with biologically interactive human albumin.[17] In patients with breast cancer, the nab paclitaxel demonstrated higher antitumor activity and clinical efficacy when compared with solvent-based paclitaxel.[20]

Choosing magnetic Fe_3O_4 nanoparticles (MNP-Fe_3O_4) as a drug delivery vector, we developed HHT-MNP-Fe_3O_4 to improve the therapeutic effect on myeloid leukemia cells and investigated its biological effects. MNP-Fe_3O_4 increased HHT sensitivity against myeloid leukemia cells by inducing apoptosis through the caspase-3 and PARP pathway. Furthermore, the animal studies also confirmed its remarkable antitumor activity in mice. Our study demonstrates the potential of HHT-MNP-Fe_3O_4 as an effective strategy for myeloid leukemia and more hematological malignancies in the clinic.

Materials and methods

Cell culture

The myeloid leukemia cell lines HL60, K562, NB4, and SHI-1 were obtained from the Shanghai Cell Culture Institute (Shanghai, People's Republic of China). All but SHI-1 cell lines were cultured in RPMI-1640 (SHI-1 cell line in Iscoves modified Dulbecco medium), containing 100 U/mL penicillin and 10% fetal bovine serum. All cell lines were incubated in a humidified atmosphere containing 5% CO_2 at 37°C. Total viable cells were assessed using the trypan blue staining.

Materials

HHT was obtained from Shaanxi Sciphar Biotechnology Co., Ltd (Shanxi Province, People's Republic of China). Oleic acid-coated iron oxide NPs were obtained from Jiangsu Key Laboratory for Biomaterials and Devices (Southeast University, Nanjing, People's Republic of China). Other reagents used included cell counting kit-8 (Sigma Chemicals, Perth, Australia), Annexin V-fluorescein isothiocyanate Apoptosis Detection Kit (KeyGEN Biotech, Nanjing, People's Republic of China), Cell Cycle Detection Kit (Beyotime Institute of Biotechnology, Jiangsu, People's Republic of China), Transwell insert chambers (Costar®; Corning Inc., Corning, NY, USA), matrigel-coated membrane inserts (BD Biosciences, San Jose, CA, USA), and 1% methylcellulose lysis buffer (RIPA lysis buffer, Beyotime Institute of Biotechnology). Monoclonal antibodies, including those for caspase-3, PARP, Mcl-1, and β-actin, were supplied by Santa Cruz Biotechnology Inc. (Dallas, TX, USA). All reagents were of analytical grade.

Preparation of HHT-MNP-Fe_3O_4

A two-step method reported previously was used for the synthesis of oleic acid-coated iron oxide NPs.[21] HHT and oleic acid-coated iron oxide NPs were dissolved in tetrahydrofuran at a ratio of 1:5 (w/w) for preparation of HHT-MNP-Fe_3O_4. The mixture was slowly added into 1% polyoxyethylene–polyoxypropylene copolymer solution under sonication, and the resulting suspension was stirred for 6 hours to evaporate tetrahydrofuran. Finally, the resulting suspension was filtered and lyophilized. The drug loaded in MNP-Fe_3O_4 was 10.71 wt% (HHT-to-iron weight ratio). The free drug was separated from loaded drug by retrodialysis method and quantified by high-performance liquid chromatography.[22,23] The morphology of MNP-Fe_3O_4 after rehydration was observed using a transmission electron microscope. The hydrodynamic diameter and size distribution of MNP-Fe_3O_4 were examined using a dynamic light scattering instrument and analyzed by

Brookhaven Instruments NanoDLS Particle Sizing Software. To determine the kinetics of HHT release from HHT-MNP-Fe_3O_4 NPs, 1 mL of the HHT-MNP-Fe_3O_4 NPs was placed into a dialysis bag (8,000–12,000 Da) and submerged into 10 mL of pH 7.4 PBS (with 0.5% Tween-80) at 37°C with stirring for 48 hours. At 12 hours, 24 hours, 36 hours, and 48 hours, 1 mL of buffer was withdrawn and replaced with the same volume of buffer. The concentration of HHT was determined by high-performance liquid chromatography.[23]

Animal model

Subcutaneous tumor model

Female athymic nude mice, aged 5 weeks and weighing 20±2 g, were purchased from the Shanghai Laboratory Animal Center, People's Republic of China. SHI-1 cells (1×10^7cells per mouse) were inoculated subcutaneously to mice at the left axilla (designated as day 0). Mice were randomly divided into four groups. Tumors were measured by a vernier caliper on alternate days and their volume (V) were calculated as $V = d^2 \times D/2$ where d and D represent the shortest and the longest diameter of the tumor in mm, respectively. When the tumor reached a mean size of 100 mm^3, the mice were injected with 2.5 mg/kg HHT or HHT-MNP-Fe_3O_4. The treatment was carried out three times without interval in 3 days by the tail vein. Tumor volume was measured at days 7, 14, 21, and 28 to evaluate the drug effect. At day 28, mice were killed and the tumors were fixed in 10% neutral formalin, desiccated, and then embedded in paraffin for hematoxylin–eosin (HE) staining. This assessment was performed by independent microscopists. This study was approved by the ethics committee and Animal Care and Use Committee of the First Affiliated Hospital of Soochow University. All operations were performed according to the International Guiding Principles for Biomedical Research involving Animals 1985.

Mice leukemia model

Four- to five-week-old BABL/C mice were inoculated with EL9611, a murine erythroleukemia cell line.[16] A dose of 5×10^6 EL9611 cells was transplanted through tail vein injection. Then, mice were randomly divided into four groups. After 7 days, treatments were continued for 3 days as described previously. At day 14, the spleen tissues were excised from the mice, fixed with 4% paraformaldehyde solution, and embedded in paraffin for immunohistochemical analysis.

Statistical analysis

Data were represented as mean ± SD of three independent experiments. The statistics of experiment results were calculated by one-way analysis of variance and Student's t-test. $P<0.05$ was chosen as significance level for all analyses performed.

Results

Physicochemical and properties of HHT-MNP-Fe_3O_4

As shown in Figure 1A, the polymeric micelles were generated by the hydrophobic interaction of the polyoxyethylene–polyoxypropylene copolymer chain and oleic acid on the surface of iron oxide NPs. The average core size of these HHT-NPs determined by transmission electron microscope was 11.2 nm (Figure 1B). The average hydrodynamic diameter of HHT-NPs for three batches determined by dynamic light scattering was 57.3±2.2 nm (Figure 1C), which covered both the core–shell and its aqueous layer. Moreover, the polydispersity index of HHT-NPs is 0.119. The drug release from NPs at 12 hours, 24 hours, 36 hours, and 48 hours was 7.2%±2.1%, 19.2%±3.5%, 26.7%±5.4%, and 46.2%±3.9%, respectively. The results show that the release rate of HHT from HHT-MNP-Fe_3O_4 NPs is very slow and a sustained release would be expected in vivo.

Effect of HHT-MNP-Fe_3O_4 on leukemia cell lines in vitro

Four cell lines (K562, HL-60, SHI-1, and NB4) were employed to test the growth inhibition and cytotoxicity of HHT-MNP-Fe_3O_4. After treating with HHT at various concentrations for 24 hours, 36 hours, and 48 hours, NB4 was the cell line most sensitive to HHT treatment (Figure 2A). The mean IC_{50} values for HHT-induced NB4 in three independent experiments were 0.022 μM, 0.014 μM, and 0.09 μM at 24 hours, 36 hours, and 48 hours, respectively (Figure 2B). So, we chose NB4 cells as the experiment subject in vitro. HHT-MNP-Fe_3O_4 demonstrated antitumor activity against NB4 cells in a dose-dependent manner (Figure 2C). Furthermore, HHT-MNP-Fe_3O_4 displayed a higher inhibition ratio compared with HHT at a dose of 0.015625–0.125 μM ($P<0.05$).

The morphological features of HE-stained NB4 were characterized under an optical microscope (Figure 3A). After treating with HHT and HHT-MNP-Fe_3O_4 at the dose of 0.015625 μM for 24 hours, there were typical apoptotic morphological changes such as formation of apoptotic bodies, nuclear fragmentation, and karyopyknosis found in NB4 cells. These apoptotic changes were more evident with HHT-MNP-Fe_3O_4 when compared with HHT alone. The ultrastructural morphology of NB4 cells was analyzed using a transmission electron microscope (Figure 3B).

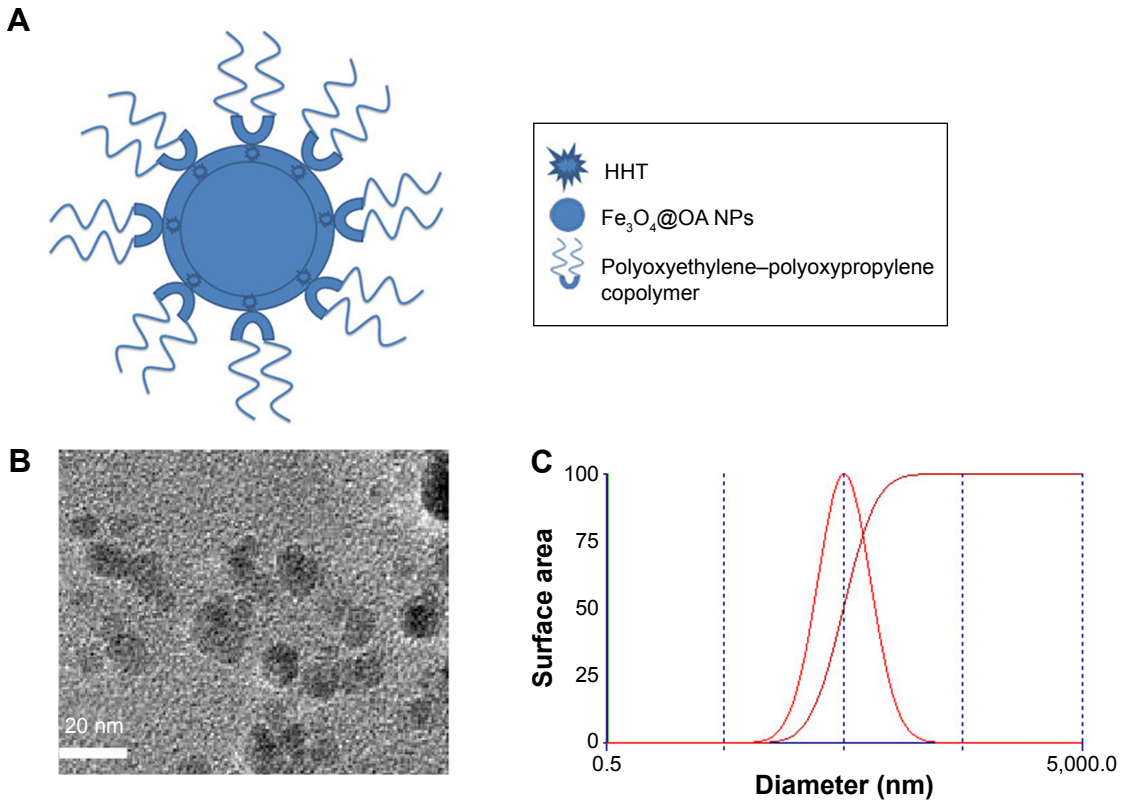

Figure 1 Construction of HHT-NPs.
Notes: (**A**) HHT-NPs that are constructed by the hydrophobic interaction between the polyoxyethylene–polyoxypropylene copolymer chain and oleic acid (OA) on the surface of iron oxide NPs; (**B**) transmission electron microscopy images of HHT-NPs after rehydration with water; and (**C**) hydrodynamic diameter of HHT-NPs after rehydration with water.
Abbreviations: HHT, homoharringtonine; NPs, nanoparticles.

The invagination of the cell membrane and visible black particles inside were observed in NB4 cells treated with MNP-Fe_3O_4, while the cellular membrane in the control group was intact. A large number of intracellular vacuoles without black particles, loosing chromatins, and swollen lysosomes were observed for NB4 cells treated with HHT. The similar phenomena but with visible black particles could be observed for NB4 cells treated with HHT-MNP-Fe_3O_4.

The apoptosis rate of NB4 cells induced by HHT-MNP-Fe_3O_4, which consisted of 0.0078125 μM HHT, was significantly higher than that induced by HHT alone at the dose of 0.0078125 μM for 24 hours (18.4% versus 10.73%; $P<0.05$; Figure 4A). This indicated that MNP-Fe_3O_4 could enhance HHT-induced apoptosis. The 24-hour HHT-MNP-Fe_3O_4 treatment resulted in a more cell arrest of NB4 cells at G0/G1 phase when compared with treatment with HHT alone. Furthermore, for the MNP-Fe_3O_4-loaded HHT group, the proportion of G0/G1 cells was increased from 47.83%±1.42% to 60.4%±1.26% ($P<0.05$; Figure 4B). Moreover, the number of colonies of NB4 cells treated with HHT-MNP-Fe_3O_4 was more than that with the HHT group (19.7±3.2 versus 25.9±4.3, $P<0.05$, Figure 4C).

Western blotting showed that higher protein levels of cleaved caspase-3 and PARP were observed in the HHT-MNP-Fe_3O_4 group when compared with the HHT group, which may account for the higher inhibition ratio of HHT-MNP-Fe_3O_4 (Figure 4D). The decreased levels of Mcl-1 protein in NB4 cells treated with HHT-MNP-Fe_3O_4 showed statistical significance compared with that with HHT alone ($P<0.05$). Therefore, the downregulation of Mcl-1 may result in marked degradation of cleaved caspase-3 and PARP.

Tumor-bearing animal models

The mean tumor volume for the mice treated with HHT-MNP-Fe_3O_4 was significantly smaller than that with HHT alone (193±26 mm^3 versus 457±100 mm^3, $P<0.05$, Figure 5A). The tumor weight for those with HHT-MNP-Fe_3O_4 was significantly smaller than with HHT alone. For the HE staining, the normal tumor cells with clear cell morphology and more chromatins were observed in the control group and the MNP-Fe_3O_4 group. It suggests a flourishing tumor growth. A large number of necrotic cells and vacuoles were observed in tumors in mice treated with HHT-MNP-Fe_3O_4,

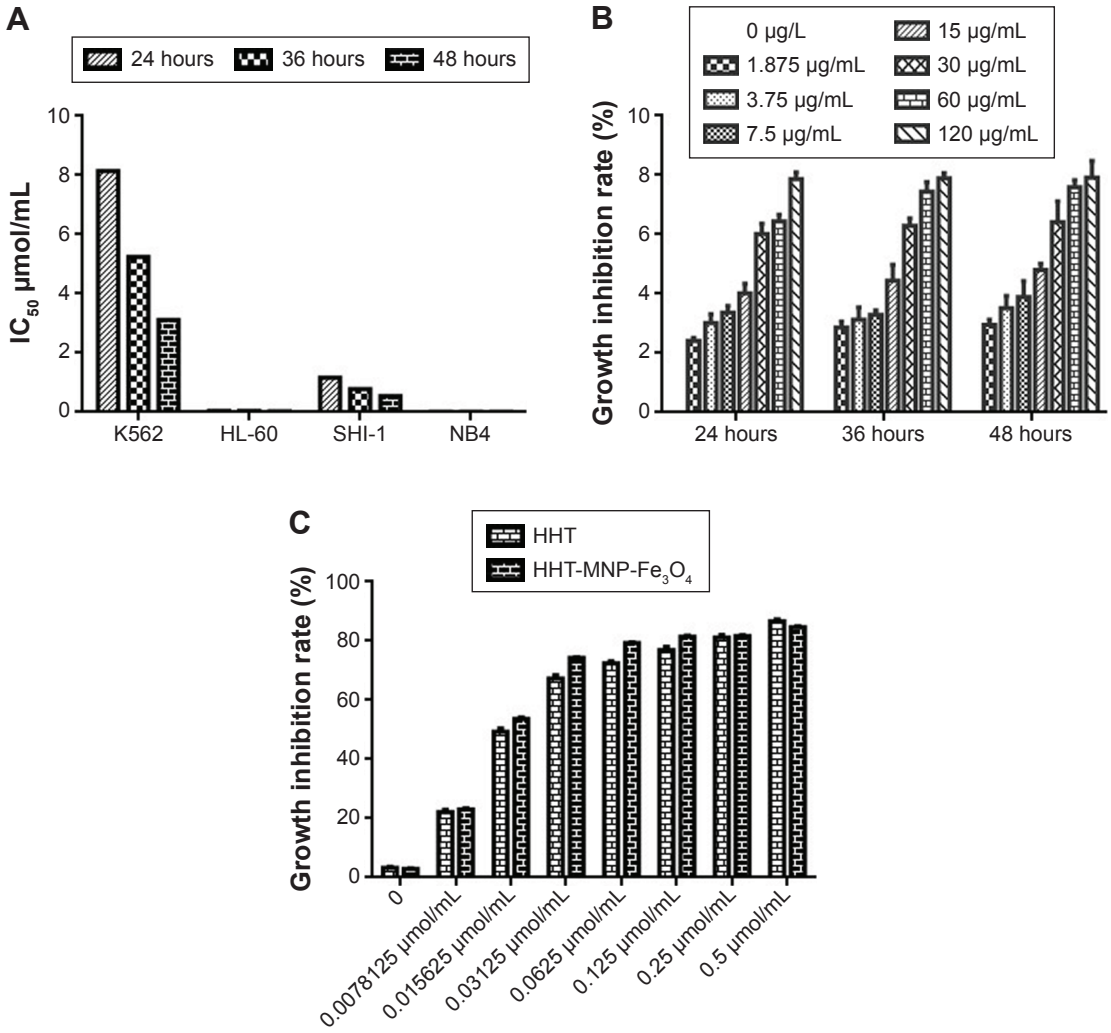

Figure 2 The inhibitory effect of different HHTs on growth of myeloblastic leukemia cell lines in vitro.
Notes: (**A**) IC_{50} of HHT on K562, HL-60, SHI-1, and NB4 in vitro; (**B**) the inhibitory effect of MNP-Fe_3O_4 on growth of NB4 for 24 hours; and (**C**) the inhibitory effect of different dosage forms of the drug on growth of NB4 for 24 hours.
Abbreviations: HHT, homoharringtonine; MNP-Fe_3O_4, magnetic Fe_3O_4 nanoparticles.

whereas only limited necrotic tumor cells could be seen in those with HHT alone (Figure 5B).

The findings with regard to the proportion of blast cells in peripheral blood from the BABL/C mice demonstrated less residual tumor cells in the HHT-MNP-Fe_3O_4 group than in the HHT group (0.09±0.05 versus 0.23±0.04, Figure 5C). Although Mcl-1 protein level in the spleen collected from the mice implied the antitumor efficacy of HHT and HHT-MNP-Fe_3O_4, the level of this protein was notably lower in the HHT-MNP-Fe_3O_4 group than in the HHT group (0.17±0.057 versus 0.31±0.061, Figure 5D). These results suggested that HHT-MNP-Fe_3O_4 had higher antitumor activity than HHT in vivo.

Discussion

HHT, a natural cephalotaxine alkaloid, has been used in the People's Republic of China for treatment of leukemia for >30 years. As reported previously, HHT in combination with Ara-C could induce a complete remission rate of 39%–60% in elderly patients with AML.[24,25] In a recent randomized Phase III trial (ChiCTR-TRC-06000054), HHT combined with cytarabine and aclacinomycin resulted in a CR rate of 73%, whereas HHT combined with cytarabine and daunorubicin in young patients with newly diagnosed AML resulted in a CR rate of 67%.[26] Because of its dramatic toxicity, the use of HHT is limited in the treatment of severe diseases. Moreover, the poor solubility results in poor bioavailability and low absorption of HHT. Meanwhile, the NPs can act as a universal drug carrier system for systemic administration of water-insoluble anticancer drugs. So, we chose MNP-Fe_3O_4 as a drug delivery vector for HHT, aiming to increase its antitumor activity in vitro and in vivo.

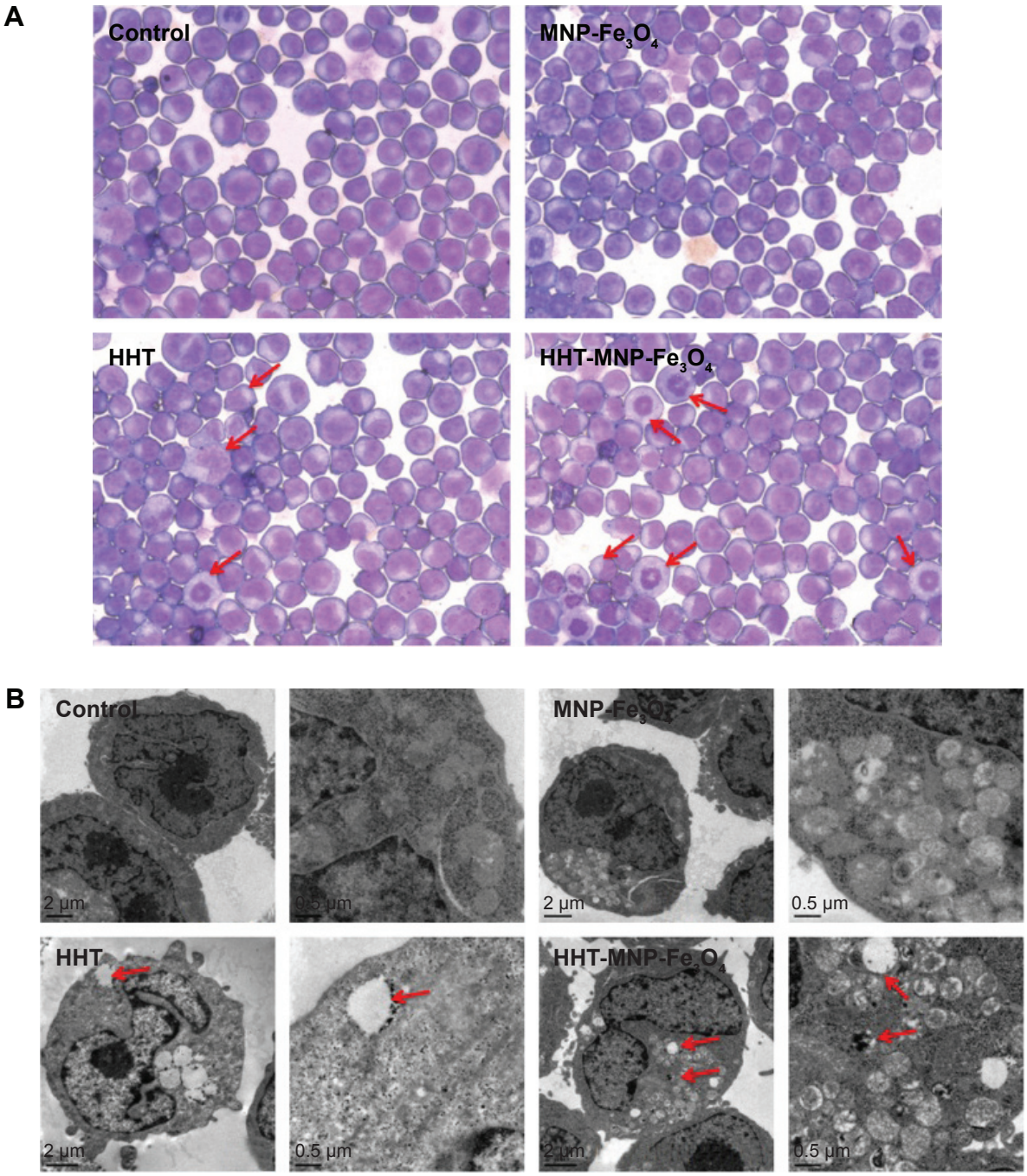

Figure 3 The morphological feature of NB4 cells after treatment with HHT-MNP-Fe_3O_4 for 24 hours in vitro.
Notes: (**A**) Photographs from optical microscope (400×, Wright staining) and (**B**) photographs from TEM. Red arrows indicate nanoparticles in the endosome vesicles.
Abbreviations: HHT, homoharringtonine; MNP-Fe_3O_4, magnetic Fe_3O_4 nanoparticles; TEM, transmission electron microscope.

The effect of growth inhibition of HHT-MNP-Fe_3O_4 was stronger than that of HHT alone as demonstrated by the significant difference between the two groups in cell proliferation and apoptosis. Apoptosis is triggered from the activation of caspases, including caspase-3, caspase-8, and caspase-9, which were situated at several key positions in the apoptotic pathways.[27] PARP, as one of the essential substrates, was activated by caspase-3 and caspase-7, which promoted the DNA strand breaks.[28] Mcl-1, as a representative prosurvival protein of the Bcl-2 family, protects tumor cells from apoptosis in the setting of hematologic malignancies.[29,30] HHT is a molecule targeting the A-site cleft of eukaryotic ribosome, which then results in the decreased expression of Mcl-1.[11,12] The introduction of MNP-Fe_3O_4 (HHT-MNP-Fe_3O_4) may improve the biological effect of HHT on Mcl-1, resulting in lower tumor cells proliferation and higher apoptosis rate than HHT alone.

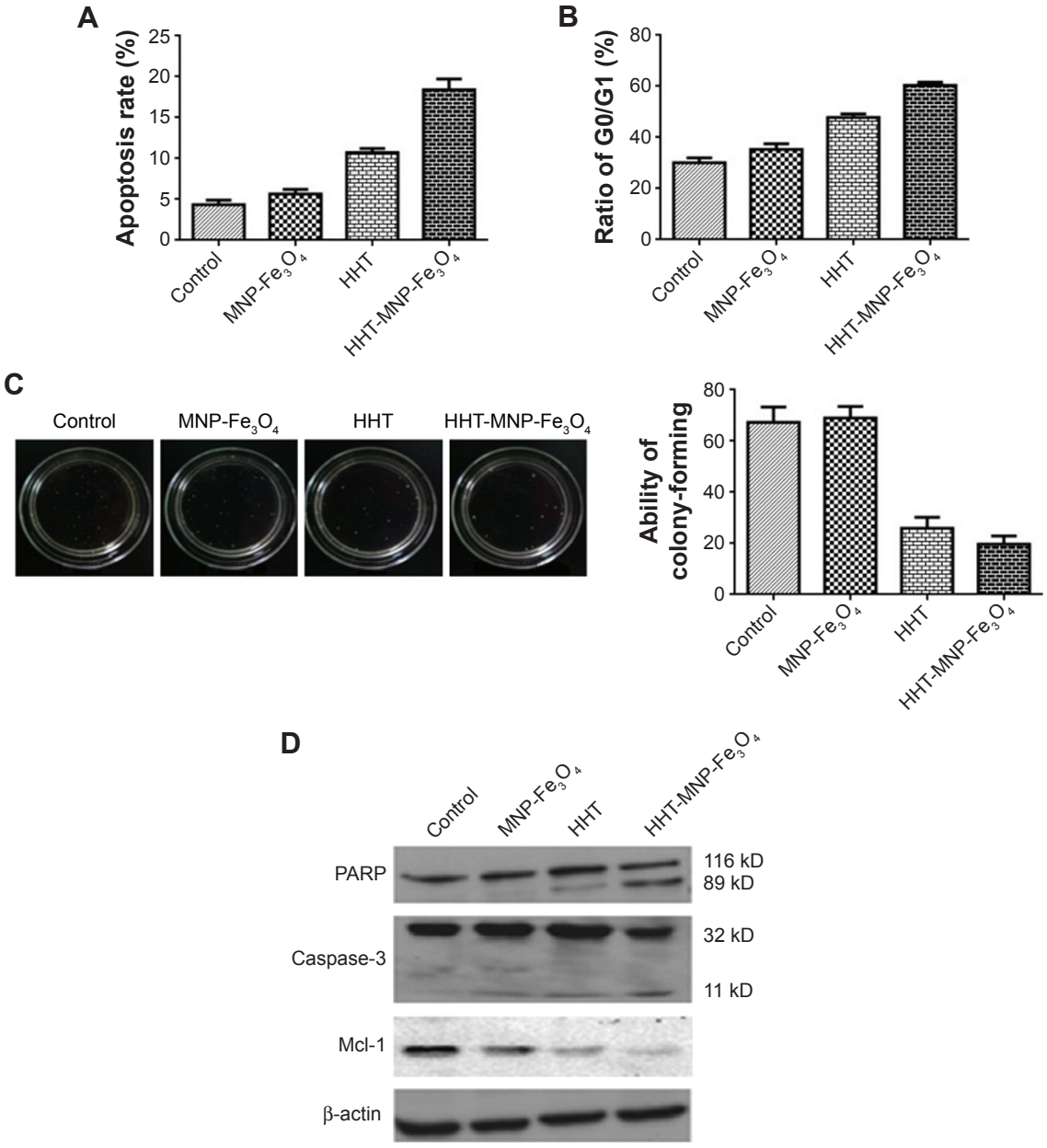

Figure 4 The impact of HHT-MNP-Fe_3O_4 on NB4 cells versus HHT.

Notes: NB4 cells were treated with different drugs: control, 1.875 μg/mL MNP-Fe_3O_4, 0.0078125 μM hhT, and 0.0078125 μM hhT +1.875 μg/mL MNP-Fe3O4. (**A**) Apoptosis and (**B**) cell cycle of NB4 cells treated with different drugs for 24 hours was detected by flow cytometry (FCM); (**C**) the ability of colony-forming of NB4 treated with different drugs for 6 hours; (**D**) the expression level of PARP, Caspase-3 and Mcl-1 protein in NB4 cells treated by different drugs was detected by western blot.

Abbreviations: HHT, homoharringtonine; Mcl-1, myeloid cell leukemia-1; MNP-Fe_3O_4, magnetic Fe_3O_4 nanoparticles; PARP, poly-ADP-ribose polymerase; FCM, flow cytometry.

Based on the earlier mentioned findings, we further investigated the antitumor efficacy in vivo of HHT-loaded NPs in tumor-bearing mice. The different magnitudes of necrosis were observed for the different dosage forms as the animals treated with HHT-MNP-Fe_3O_4 exhibited larger necrotic area than those with HHT alone. Immunohistochemical study showed that the Mcl-1-stained cells from the mice in the HHT-MNP-Fe_3O_4 group were fewer than those from the controls receiving blank MNP-Fe_3O_4 or HHT alone. The earlier mentioned data confirmed that the expression of Mcl-1 was lower in the tumor tissue treated with HHT-MNP-Fe_3O_4, which was consistent with the result of Western blotting. The superior anticancer effect of HHT-MNP-Fe_3O_4 might be associated with the stability of NPs in blood circulation, slow release to tumor site, the effective cellular uptake, and cooperative effect of HHT and NPs.

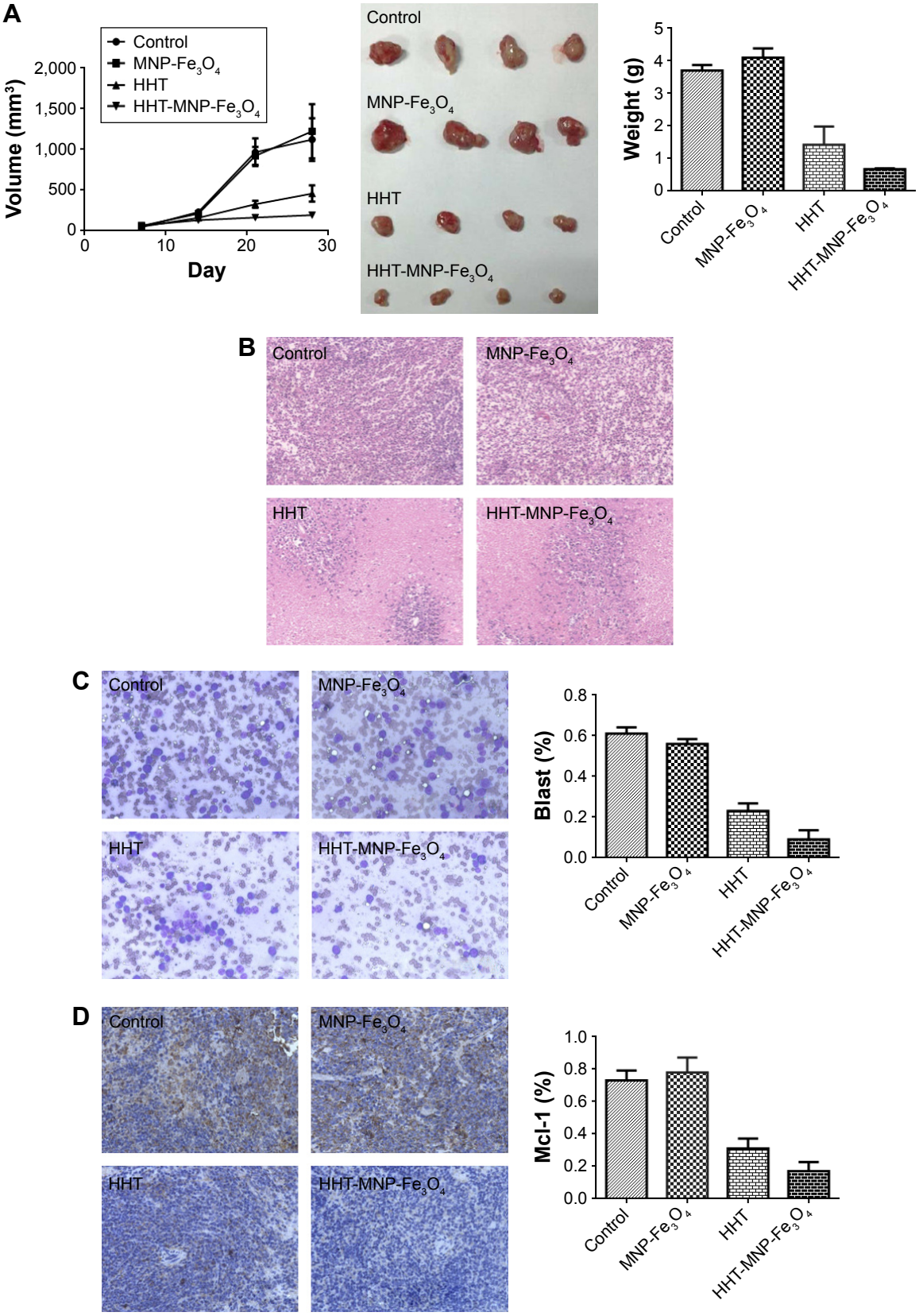

Figure 5 The impact of HHT-MNP-Fe_3O_4 on SHI-1 cells versus HHT in vivo.

Notes: (**A**) Tumor volume and body weight changes after anticancer treatment with different drug formulations in the subcutaneous model; (**B**) histological assay of tumors of SHI-1 tumor-bearing mice that received different treatments; (HE, 40× magnifications); (**C**) the proportion of blast in the peripheral blood of erythroleukemia implanted in BABL/C mice with treatments of different drug strategies (400×, Wright staining); (**D**) images of histological changes of different drug strategies in treatments of erythroleukemia implanted in BABL/C mice model. Brown and blue stains represent Mcl-1 and nuclei in immunohistochemical assay, respectively.

Abbreviations: HE, hematoxylin–eosin; HHT, homoharringtonine; Mcl-1, myeloid cell leukemia-1; MNP-Fe_3O_4, magnetic Fe_3O_4 nanoparticles.

The toxicity of HHT-MNP-Fe_3O_4 may cause some concern. However, in most studies about its in vivo toxicity, Fe_3O_4 NPs have been shown to be associated with low toxicity in the human body. It is primarily due to the fact that they can be degraded and cleared from circulation by the endogenous iron metabolic pathways. Iron released from NPs is metabolized in the liver and subsequently used in the formation of red blood cells or excreted via kidneys.[31] A study comparing several metal oxide NPs demonstrated iron oxide NPs to be safe and noncytotoxic $<$100 mg/mL.[32] Another study on normal, glial, and breast cancer cells revealed that the toxicity of Fe_3O_4 NPs coated with a bipolar surfactant is concentration dependent, with the particles being nontoxic in the concentration range of 0.1–10 mg/mL, whereas cytotoxic at 100 mg/mL.[33] Therefore, it is possible to find a safe concentration range for Fe_3O_4 NPs without triggering adverse cellular response.

Conclusion

We designed a drug delivery vector for HHT. HHT-MNP-Fe_3O_4 had cooperative effect in suppression of tumor cell growth both in vivo and in vitro. The HHT-MNP-Fe_3O_4 could enhance the therapeutic efficiency by reducing the expression of Mc-1 and activating caspase-3 and PARP. Here, we pay attention to the potential of MNP-Fe_3O_4 and HHT, which can enhance the antitumor effect, and hope the designed anticancer drugs based on this research can be used in future clinical practice. Moreover, our study may provide a promising platform of the codelivery system as a component of combination therapy in the treatment of hematological malignancies.

Acknowledgments

This study was supported by National Basic Research Program 973 of China (No 2011CB933500), the Priority Academic Program Development of Jiangsu Higher Education Institutions, National Natural Science Foundation of China (No 81473160), the Basic Research Program of Jiangsu Province (Natural Science Foundation, No BK20151422), Fundamental Research Funds for the Central Universities (No 2242014R30013 and No 2242016K40033), and Jiangsu Province Natural Science Fund (BE2015639).

Disclosure

The authors report no conflicts of interest in this work.

References

1. Grem JL, Cheson BD, King SA, Leyland-Jones B, Suffness M. Cephalotaxine esters: anti-leukemic advance or therapeutic failure? *J Natl Cancer Inst*. 1988;80(14):1095–1103.
2. Cephalotaxus Research Coordinating Group. Cephalotaxine esters in the treatment of acute leukemia. A preliminary clinical assessment. *Chin Med J (Engl)*. 1976;2:263–272.
3. Powell RG, Weisleder D, Smith CR Jr. Antitumor alkaloids for *Cephalataxus harringtonia*: structure and activity. *J Pharm Sci*. 1972;61(8):1227–1230.
4. O'Brien S, Kantarjian H, Keating M, et al. Homoharringtonine therapy induces responses in patients with chronic myelogenous leukemia in late chronic phase. *Blood*. 1995;86(9):3322–3326.
5. O'Brien S, Kantarjian H, Koller C, et al. Sequential homoharringtonine and interferon-alpha in the treatment of early chronic phase chronic myelogenous leukemia. *Blood*. 1999;93(12):4149–4153.
6. Druker BJ, Guilhot F, O'Brien SG, et al; IRIS Investigators. Five-year followup of patients receiving imatinib for chronic myeloid leukemia. *N Engl J Med*. 2006;355(23):2408–2417.
7. Druker BJ, Tamura S, Buchdunger E, et al. Effects of a selective inhibitor of the Abl tyrosine kinase on the growth of Bcr-Abl positive cells. *Nat Med*. 1996;2(5):561–566.
8. Chen Y, Hu Y, Michaels S, Segal D, Brown D, Li S. Inhibitory effects of homoharringtonine on leukemic stem cells and BCR-ABL induced chronic myeloid leukemia and acute lymphoblastic leukemia in mice. *Leukemia*. 2009;23(8):1446–1454.
9. Yinjun L, Jie J, Weilai X, Xiangming T. Homoharringtonine mediates myeloid cell apoptosis via up-regulation of pro-apoptotic bax and inducing caspase-3-mediated cleavage of poly (ADP-ribose) polymerase (PARP). *Am J Hematol*. 2004;76(3):199–204.
10. Lou YJ, Qian WB, Jin J. Homoharringtonine induces apoptosis and growth arrest in human myeloma cells. *Leuk Lymphoma*. 2007;48(7):1400–1406.
11. Gürel G, Blaha G, Moore PB, Steitz TA. U2504 determines the species specificity of the A-site cleft antibiotics: the structures of tiamulin, homoharringtonine, and bruceantin bound to the ribosome. *J Mol Biol*. 2009;389(1):146–156.
12. Tang R, Faussat AM, Majdak P, et al. Semisynthetic homoharringtonine induces apoptosis via inhibition of protein synthesis and triggers rapid myeloid cell leukemia-1 down-regulation in myeloid leukemia cells. *Mol Cancer Ther*. 2006;5(3):723–731.
13. Stewart JA, Krakoff IH. Homoharringtonine: a phase I evaluation. *Invest New Drugs*. 1985;3(3):279–286.
14. Whitacre MY, Van Echo DA, Applefeld M, et al. Phase I study of homoharringtonine (NSC 141-633). *Proc Am Soc Clin Oncol*. 1985;26:359.
15. Werle M. Natural and synthetic polymers as inhibitors of drug efflux pumps. *Pharm Res*. 2008;25(3):500–511.
16. Duncan R. Polymer conjugates as anticancer nanomedicines. *Nat Rev Cancer*. 2006;6(9):688–701.
17. Ferrari M. Cancer nanotechnology: opportunities and challenges. *Nat Rev Cancer*. 2005;5(3):161–171.
18. Zhang R, Wang X, Wu C, et al. Synergistic enhancement effect of magnetic nanoparticles on anticancer drug accumulation in cancer cells. *Nanotechnology*. 2006;17(14):3622–3626.
19. Brigger I, Dubernet C, Couvreur P. Nanoparticles in cancer therapy and diagnosis. *Adv Drug Deliv Rev*. 2002;54(5):631–651.
20. John TA, Vogel SM, Tiruppathi C, Malik AB, Minshall RD. Quantitative analysis of albumin uptake and transport in the rat microvessel endothelial monolayer. *Am J Physiol Lung Cell Mol Physiol*. 2003; 284(1):L187–L196.
21. Jain TK, Morales MA, Sahoo SK, Leslie-Pelecky DL, Labhasetwar V. Iron oxide nanoparticles for sustained delivery of anticancer agents. *Mol Pharm*. 2005;2(3):194–205.
22. Xiong F, Zhu JB, Wang W, Hua XB. Determination of entrapment efficiency of breviscapinenanoliposomes. *Acta Pharm Sin*. 2004;39(9):755–757.
23. Yang M, Yang C, Ma J, Bian S, Xue Y. Determination of the content of homoharringtonine in serum by HPLC. *Chin J Pharm Anal*. 1999; 19(3):147–149.
24. Huang BT, Zeng QC, Yu J, Liu XL, Xiao Z, Zhu HQ. High-dose homoharringtonine versus standard-dose daunorubicin is effective and safe as induction and postinduction chemotherapy for elderly patients with acute myeloid leukemia: a multicenter experience from China. *Med Oncol*. 2012;29(1):251–259.

25. Wang J, Lü S, Yang J, et al. A homoharringtonine-based induction regimen for the treatment of elderly patients with acute myeloid leukemia: a single center experience from China. *J Hematol Oncol*. 2009;2:32.
26. Jin J, Wang JX, Chen FF, et al. Homoharringtonine-based induction regimens for patients with de-novo acute myeloid leukaemia: a multicentre, open-label, randomised, controlled phase 3 trial. *Lancet Oncol*. 2013; 14(7):599–608.
27. Reed JC, Pellecchia M. Apoptosis-based therapies for hematologic malignancies. *Blood*. 2005;106(2):408–418.
28. Bressenot A, Marchal S, Bezdetnaya L, Garrier J, Guillemin F, Plénat F. Assessment of apoptosis by immunohistochemistry to active caspase-3, active caspase-7, or cleaved PARP in monolayer cells and spheroid and subcutaneous xenografts of human carcinoma. *J Histochem Cytochem*. 2009;57(4):289–300.
29. Pan J, Quintás-Cardama A, Manshouri T, et al. The novel tyrosine kinase inhibitor EXEL-0862 induces apoptosis in human FIP1L1-PDGFR-α-expressing cells through caspase-3-mediated cleavage of Mcl-1. *Leukemia*. 2007;21:1395–1404.
30. Dasmahapatra G, Yerram N, Dai Y, Dent P, Grant S. Synergistic interactions between vorinostat and sorafenib in chronic myelogenous leukemia cells involve Mcl-1 and p21CIP1 down-regulation. *Clin Cancer Res*. 2007;13(14):4280–4290.
31. Ankamwar B, Lai TC, Huang JH, et al. Biocompatibility of Fe(3)O(4) nanoparticles evaluated by in vitro cytotoxicity assays using normal, glia and breast cancer cells. *Nanotechnology*. 2010;21(7):75102.
32. Karlsson HL, Gustafsson J, Cronholm P, Möller L. Size-dependent toxicity of metal oxide particles: a comparison between nano- and micrometer size. *Toxicol Lett*. 2009;188(2):112–118.
33. Karlsson HL, Cronholm P, Gustafsson J, Möller L. Copper oxide nanoparticles are highly toxic: a comparison between metal oxide nanoparticles and carbon nanotubes. *Chem Res Toxicol*. 2008;21(9): 1726–1732.